Silicon (2023) 15:305–319
https://doi.org/10.1007/s12633-022-02004-y

ORIGINAL PAPER

Element Transfer Investigations on Silica Based Submerged Arc Welding Fluxes

Lochan Sharma[1] · Rahul Chhibber[2] · Vijay Kumar[2] · Waris Nawaz Khan[2]

Received: 4 February 2022 / Accepted: 20 June 2022 / Published online: 19 July 2022

Abstract
By using laboratory developed agglomerated basic fluxes a study has been carried out to predict the element transfer across the series of bead on plate weld deposits in submerged arc welding process (SAW). With the application of mathematical experiments of mixture design approach different statistical model were developed in terms of flux constituents. Using twenty one basic submerged arc welding fluxes a series of bead on plate weld deposits were made at constant welding parameters. Twenty one submerged arc welding fluxes were prepared as per mixture design approach for CaF_2-SiO_2-CaO & SiO_2-CaF_2-Al_2O_3 flux system. Results indicates that there was predominant effect on weld metal carbon, silicon, manganese, sulphur, phosphorous, molybdenum and chromium contents. The weld bead carbon content for all the fluxes has been increased while it is lower than that of base metal. Individual flux ingredients CaO, SiO_2, CaF_2 and Al_2O_3 incresars the delta carbon content and shows synergistic effect on it while binary mixture interations such as CaO.SiO_2, CaO.CaF_2, CaO.Al_2O_3, SiO_2.CaF_2 and CaF_2.Al_2O_3 gives the negative effect on delta carbon content.

Keywords API X70 steel · Basic flux composition · SAW · Delta quantities · Mixture design approach

1 Introduction

In 70s and 80s due to the advancement in the steel manufacturing processes, such as ladle processing for alloy additions, basic oxygen furnace production, continuous slab casting and vacuum degassing pushed pipe manufacturer to produce stronger and technically challenging steels. The line pipe grade most commonly used evolved rapidly from X52 to X60 and then X65 to X70 through 1990 with these technologies. In 1993, a new grade (X80) to the pipeline family came with parallel development in X70. The need for the development of X70 and X80 grade was that alloy system used for X65 production consisting of titanium stabilised carbon manganese steel strengthened with niobium and vanadium which had a limited ability to be extended to higher strengths. Carbon equivalent approaches an unacceptable level as strength increases to the addition of higher alloy content. For this, vanadium was replaced by molybdenum, strong carbide former and the very effective strengthening agent was added [1, 2]. To provide higher atmospheric corrosion protection than normal steels, a wide variety of alloy steels manufactured for enhancing mechanical properties known as HSLA steels which are frequently used as line pipe steels. HSLA steels are extensively used in many oil and gas transportation applications [3].Welding (eg. arc welding) is often required for manufacturing such steel structures [4, 5]. Among them submerged arc welding offers several advantages in welding of structural steels such as high toughness in the weld zone due to slow cooling involved. Quality and performance of welding fluxes has been assessed based on two parameters such as welding process stability and weld bead appearance which are the integral part of it. Both theses parameters primarily depends upon the type of coating/flux and filler wire used. There is much similarity in the behaviour of SAW welding fluxes with that of coating mixture used in covered

✉ Waris Nawaz Khan
khan.3@iitj.ac.in

Lochan Sharma
lochan.e9455@cumail.in

Rahul Chhibber
rahul_chhibber@iitj.ac.in

Vijay Kumar
vijay.4@iitj.ac.in

1 University Centre of Research and Development, Chandigarh University, Gharuan, Punjab, India

2 MED, IIT Jodhpur, Jodhpur, India

electrodes in case of shielded metal arc welding (SMAW). Due to tremendous inherent features such as smooth finish, high quality, deep penetration and joining of thicker sections submerged arc welding process is frequently utilized in the pipeline industry. In submerged arc welding process, flux mixture disintegrated in arc column while at same time filler wire melted and transferred into the weld region resulting in the formation slag which prevents the molten weld region from atmospheric environment [6, 7]. Due to metallurgical reactions, there are some chances of loss of filler metal by oxidation or evaporation while some of the flux constituents may possible to enter in the weld pool region. Final weld metal composition is mainly decided by how well metal transfer takes place during submerged arc welding process. Metallurgical as well as mechanical properties of submerged arc weldments mainly depends upon the element transfer, flux composition, joint geometry and filler wire composition. During welding, different metallic oxides dissociates in the arc region and promote the phase transformation. In submerged arc welding, accicular ferrite phase is formed due to the interaction of various oxides in the weld pool at high temperature and this particular phase is responsible for enhancing the impact strength of SAW weldments. Physicochemical and thermophysical properties of submerged arc fluxes widely affected by cooling rate, slag behaviour and final weld joint properties such as tensile strength, impact toughness etc. during submerged arc welding [8–13]. Adequate weld joint is required to fulfil the specified strength of line pipe steel as specified during the manufacturing process. To solve this problem, combined electrode manual welding technique was used. For large practical applications this combined electrode manual welding and SAW technique frequently utilized in the industry. During submerged arc welding, melting of both parent metal as well as filler wire take place under the blanket of agglomerated fluxes. Oxidation as well as contamination of the weld pool has been protected by the outer layer of the flux formed in the form of slag on the weld pool. Due to this total heat input is fully concentrated into the weld joint. Flux not only protect the weld pool but it also act as a cleansing agent in submerged arc welding process [14–19]. This paper presents an overview of the role of welding flux constituents and their interactions on the delta (Δ) element transfer during SAW process.

2 Experimentation

2.1 Flux Matrix Design

To predict the influence of basic flux constituents on the element transfer due to flux, twenty one basic fluxes were utilized. By changing the composition of 4 basic flux constituents **Al_2O_3, CaF_2, SiO_2 and CaO** and keeping the bentonite content fixed these fluxes were prepared as shown in Table 1.

Table 1 Design of flux matrix

Exp. No		Design points	Ingredients of flux constituents (wt.%)			
	B_{flux}		CaO	SiO_2	CaF_2	Al_2O_3
1	f1	V	40.1	10.1	25.1	10.1
2	f2	V	40.1	15.1	25.1	5.1
3	f3	V	40.1	18.70	18.70	7.4
4	f4	V	30.1	25.1	25.1	5.1
5	f5	V	36.44	21.44	21.44	5.1
6	f6	V	35.38	20.38	20.38	7.4
7	f7	C_E	40.1	25.1	10.1	10.1
8	f8	C_E	33.57	18.57	25.1	7.4
9	f9	C_E	35.1	20.1	20.1	10.1
10	f10	C_E	33.57	25.1	18.05	7.4
11	f11	C_E	25.1	25.1	25.1	10.1
12	f12	C_E	40.1	25.1	15.1	5.1
13	f13	C_E	32.4	25.1	17.4	10.1
14	f14	C_E	32.4	17.4	25.1	10.1
15	f15	C_E	40.1	12.5	25.1	7.4
16	f16	C_E	40.1	17.4	17.4	10.1
17	f17	C_E	40.1	25.1	12.5	7.4
18	f18	C_E	35.1	25.1	20.1	5.1
19	f19	P_C	40.1	20.1	20.1	5.1
20	f20	P_C	27.5	25.1	25.1	7.4
21	f21	O_C	35.1	20.1	25.1	5.1

According to the extreme vertices design approach chemical composition of fluxes were decided. To decide the suitable range of basic fluxes two ternary phase diagrams were used as shown in Fig. 1a-b. Minimum and maximum range of flux constituents is shown by Eq. 1 with total maximum constrained is 90%. Using laboratory prepared basic fluxes 21 multi-pass weld beads were developed on API X70 pipeline steel. Fig. 2a-b represents the series of bead on plate experimentation performed on SAW machine. Table 2 represents the chemical composition of parent metal and filler wire. API X70 base plates was utilized to develop 21 weld bead deposits using 3.2 mm electrode wire with DCEP polarity. Different trial runs were carried out to select the optimum parameters. Different trials were carried out to assess the slag detachability as well as bead profiles. Qualitative analysis such as porosity and slag detachability of different beads was assessed at low, medium & high scale. Based on the pretrails current (300–470 amp), voltage (20–34 V) and welding speed (5–10 in./min) range were selected. Equation 2 was used to calculate the heat input of welded specimen.

$$\begin{aligned} 25.1 &\le \mathbf{CaO}(t1) \le 40.1 \\ 10.1 &\le \mathbf{SiO_2}\ (t2) \le 25.1 \\ 10.1 &\le \mathbf{CaF_2}(t3) \le 25.1 \\ 5.1 &\le \mathbf{Al_2O3}\ (t4) \le 10.1 \\ &\textstyle\sum_{i=1}^{4} t_i = 90 \end{aligned} \tag{1}$$

$$\text{Heat Input} = (60\ \text{x Amps x volts})/(1000\ \text{x Travel Speed})\text{KJ/inch} \tag{2}$$

Where Travel speed = Length of weld / Time of weld in inch/min.

Length of weld bead = 250 mm or 9.85 in.; Time of weld = 60 sec.

Travel speed = 9.85 in./min.

I = 450 amp; V = 32 V;

Heat Input = (60 sec/ min × 450 amp × 32 V) / (1000 j/KJ × 9.85 in./min).

Heat Input = 87.7 KJ/min.

During submerged arc welding process, heat transfer rate, reaction rate and diffusion rate strongly depends on the physical properties of fluxes. Thermophysical and physicochemical properties such as thermal conductivity, thermal diffusivity, specific heat, density and viscosity affects the weld metal mechanical properties after solidification of weld joint. In present study, hot disk technique was used to find the physical properties such as thermal conductivity, thermal diffusivity and specific heat of twenty one submerged arc welding fluxes. Thermogravimetric analysis (TGA) was also carried out of twenty one submerged arc welding fluxes to find their thermal stability. Table 3 shows the thermal conductivity, thermal diffusivity and specific heat variation for twenty one submerged arc welding fluxes.

2.2 Element Transfer Evaluation in Series of Bead on Plate Weld Deposits

Equation 1 is used to evaluate the dilution (D) due to parent metal as well due to filler wire (1-D) in submerged arc welding process. After cutting the bead specimen general metallurgical polishing and etching operation was used to find the weld bead profile. Digital planimeter & profile projector was used to measure the area of bead profile & filler wire. Equation 2 was used to find the expected weld metal dilution content. To observe the element transfer due to flux a delta quantity (Δ) was used which is obtained by

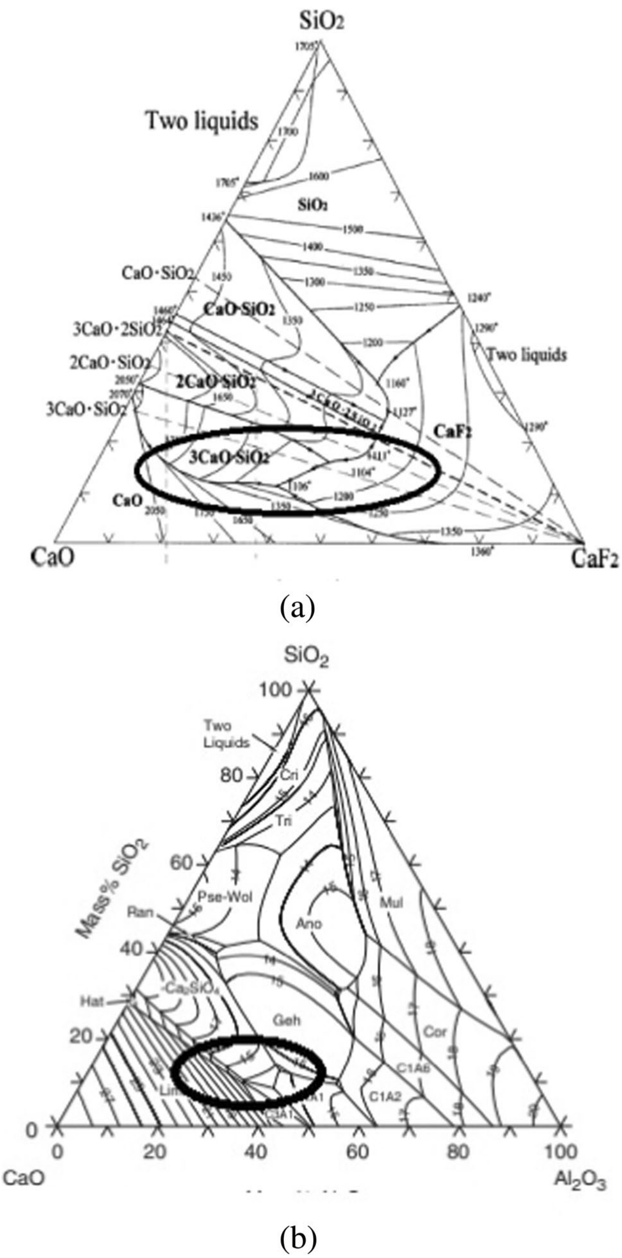

Fig. 1 **a-b**: Ternary phase diagram [20–22]

Fig. 2 **a-b**: Series of bead on plate experimentation

the difference of expected and observed weld metal content. Transfer of elements from slag to weld shows the gain of elements and (Δ) quantity is taken as positive value. While transfer of elements from weld to slag should be read as loss of elements and in this case (Δ) quantity is taken as negative value. Table 4 represents the dilution values and chemical composition of weld bead deposits. Table 5 represents the observed as well as (Δ) transfer quantities by flux.

$$\text{Dilution (D)} = \text{Parent metal Area/Parent mental area} + \text{Fused area of filler wire} \quad (3)$$

$$\text{Expected weld content} = \text{D x Parent metal element content} + (1 - \text{D}) \text{ Filler wire element content} \quad (4)$$

3 Results and Discussion

3.1 Formation of Regression Models for the Change of Element Transfer

Least square regression equations (Eqs. 3–9) in terms of percentage composition of flux constituents were formed by using observed values of chemical composition from experimentation. Second and third order regression models were formed in terms of primary, secondary & ternary flux mixture interactions. ANOVA has been used to check the adequacy of the predicted equations. By finding the F and P values at 95% confidence level the whole mixture models has been verified for linear, quadratic and cubic square models [23]. Figure 3 represents the predicted vs. actual values for all the responses and it has been observed from the plots that predicted values are in close agreement with the observed values for most of the responses in series of weld bead deposit composition. Table 6 represents the ANOVA results with R^2 values for all the responses.

$$\begin{aligned}\Delta_C = {} & +5.0540E-003.CaO + 0.018657.SiO_2 \\ & + 9.28578E-003.CaF_2 + 0.16137.Al_2O_3 \\ & - 3.52356E-004 \text{ x } CaO.SiO_2 - 1.15676E \\ & - 004 \text{ x } CaO.CaF_2 - 3.16130E-003 \text{ x } CaO.Al_2O_3 \\ & - 4.14373E-004 \text{ x } SiO_2.CaF_2 - 4.86033E \\ & - 003 \text{ x } SiO_2.Al_2O_3 - 3.16605E-003 \text{ x } CaF_2.Al_2O_3 \\ & - 8.05615E-006 \text{ x } CaO.SiO_2.CaF_2 + 7.33020E \\ & - 005 \text{ x } CaO.SiO_2.Al_2O_3 + 3.10802E-005 \text{ x } CaO.CaF_2.Al_2O_3 \\ & + 6.29696E-005 \text{ x } SiO_2.CaF_2.Al_2O_3\end{aligned} \quad (5)$$

$$\begin{aligned}\Delta_{Si} = {} & -0.014189.CaO - 0.011904.SiO_2 - 9.33500E \\ & - 003.CaF_2 - 0.26327.Al_2O_3 + 3.81194E-004 \text{ x } CaO.SiO_2 \\ & + 4.47053E-004 \text{ x } CaO.CaF_2 + 3.97103E-003 \text{ x } CaO.Al_2O_3 \\ & + 6.64693E-004 \text{ x } SiO_2.CaF_2 + 4.95423E-003.CaF_2.Al_2O_3 \\ & + 3.20824E-003xCaF_2.Al_2O_3\end{aligned} \quad (6)$$

$$\begin{aligned}\Delta_{Mn} = {} & 0.12898.CaO + 0.19959.SiO_2 + 0.55037.CaF_2 \\ & + 2.99099.Al_2O_3 - 2.87518E-003 \text{ x } CaO.SiO_2 \\ & - 0.011982 \text{ x } CaO.CaF_2 - 0.055466 \text{ x } CaO.Al_2O_3 \\ & - 0.014809 \text{ x } CaO.CaF_2 - 0.059968 \text{ x } SiO_2.Al_2O_3 \\ & - 0.095758 \text{ x } CaF_2.Al_2O_3 - 4.16843E-003 \text{ x } CaO.SiO_2.CaF_2 \\ & + 3.66188E-004 \text{ x } CaO.SiO_2.Al_2O_3 + 1.33205E \\ & - 003xCaO.CaF_2.Al_2O_3 + 1.46136E-003xSiO_2.CaF_2.Al_2O_3\end{aligned} \quad (7)$$

$$\begin{aligned}\Delta_P = {} & 1.57943E-003.CaO + 4.23221E-003.SiO_2 \\ & + 2.80411E-003.CaF_2 - 0.025027.Al_2O_3 - 1.54113E \\ & - 004 \text{ x } CaO.SiO_2 - 1.43295E-004 \text{ x } CaO.CaF_2 \\ & + 3.81462E-004 \text{ x } CaO.Al_2O_3 - 2.73396E-004 \text{ x } SiO_2.CaF_2 \\ & + 4.06569E-004 \text{ x } SiO_2.Al_2O_3 + 5.32063E-004 \text{ x } CaF_2.Al_2O_3 \\ & + 9.02175E-006 \text{ x } CaO.SiO_2.CaF_2 - 3.23337E-006 \text{ x } CaO.SiO_2.Al_2O_3 \\ & - 3.11754E-006 \text{ x } CaO.CaF_2.Al_2O_3 - 4.59141E-006 \text{ } SiO_2.CaF_2.Al_2O_3\end{aligned} \quad (8)$$

Table 2 Chemical composition of base metal and filler wire

Material	*C*	*Si*	*Mn*	*P*	*S*	*Mo*	*Ni*	*Cr*	*Fe*
PM (X70)	0.063	0.321	1.640	0.007	0.001	0.001	0.318	0.006	97.5
FW (EA2TiB)	0.029	0.088	0.871	0.010	0.007	0.216	0.084	0.032	98.4

Table 3 Physical Properties of submerged arc welding fluxes

Flux	Density (g/cm^3)	Thermal conductivity (W/mK)	Thermal diffusivity (mm^2/s)	Specific heat (MJ/m^3K)	Percentage weight change
F1	1.312	0.145	0.207	0.702	0.924
F2	1.372	0.122	0.221	0.551	1.828
F3	1.398	0.139	0.245	0.568	1.388
F4	1.421	0.134	0.190	0.705	0.615
F5	1.511	0.150	0.273	0.549	0.495
F6	1.411	0.135	0.206	0.656	4.261
F7	1.571	0.138	0.219	0.629	1.688
F8	1.537	0.157	0.329	0.478	1.028
F9	1.492	0.141	0.195	0.725	4.060
F10	1.500	0.207	0.403	0.513	0.320
F11	1.521	0.195	0.322	0.605	0.461
F12	1.565	0.247	0.365	0.677	0.567
F13	1.581	0.166	0.295	0.564	1.470
F14	1.531	0.172	0.410	0.419	1.258
F15	1.510	0.189	0.507	0.373	1.181
F16	1.580	0.178	0.297	0.598	0.823
F17	1.544	0.175	0.338	0.519	1.088
F18	1.590	0.161	0.293	0.549	0.569
F19	1.600	0.173	0.257	0.674	0.794
F20	1.580	0.183	0.351	0.523	0.645
F21	1.522	0.158	0.278	0.568	0.578

$$\begin{aligned}\Delta_S = & -1.58023E-003.CaO - 1.54178E-003.SiO_2 \\ & - 1.03663E-003.CaF_2 - 0.011154.Al_2O_3 + 5.70516E \\ & - 005 \text{ x } CaO.SiO_2 + 4.89377E-005 \text{ x } CaO.CaF_2 \\ & + 2.02411E-004\ CaO.Al_2O_3 + 2.76005E-005 \text{ x } SiO_2.CaF_2 \\ & + 1.76761E-004 \text{ x } SiO_2.Al_2O_3 + 1.41389E-004 \text{ x } CaF_2.Al_2O_3\end{aligned} \tag{9}$$

$$\begin{aligned}\Delta_{Mo} = & 0.051253 \text{ x } CaO + 0.048205 \text{ x } SiO_2 - 0.11215 \text{ x } CaF_2 \\ & - 0.38922 \text{ x } Al_2O_3 + 3.99609E-003 \text{ x } CaO \text{ x } CaF_2 \\ & + 0.010833\text{x } CaO \text{ x } Al_2O_3 + 0.017096 \text{ x } CaF_2 \text{ x } Al_2O_3 \\ & - 4.14899E-004\ CaO \text{ x } CaF_2 \text{ x } Al_2O_3\end{aligned} \tag{10}$$

$$\begin{aligned}\Delta_{Ni} = & -0.010617.CaO - 0.015769.SiO_2 - 0.097877.CaF_27 \\ & + 0.27264.Al_2O_3 + 7.18723E-004 \text{ x } CaO.SiO2 \\ & + 2.78192E-003 \text{ x } CaO.CaF2 - 6.92751E-003\ CaO.Al2O3 \\ & + 4.32627E-003 \text{ x } SiO2.CaF2 - 0.010408 \text{ x } SiO2.Al_2O_3 \\ & - 1.24350E-004.CaO.SiO_2.CaF_2 + 2.65238E-004 \text{ x } CaO.SiO_2.Al_2O_3\end{aligned} \tag{11}$$

$$\begin{aligned}\Delta_{Cr} = & 6.39823E-003.CaO + 8.17831E-003.SiO_2 \\ & + 0.045370.CaF_2 + 7.77736E-003.Al_2O_3 \\ & - 1.95943E-004 \text{ x } CaO.SiO_2 - 1.15971E \\ & - 003 \text{ x } CaO.CaF_2 + 2.15963E-004 \text{ x } CaO.Al_2O_3 \\ & - 1.57207E-003 \text{ x } SiO_2.CaF_2 + 9.61640E-004 \text{ x } SiO_2.Al_2O_3 \\ & - 3.19492E-003 \text{ x } CaF_2.Al_2O_3 + 2.93103E-005 \text{ x } CaO.SiO_2.CaF_2 \\ & - 5.55674E-005 \text{ x } CaO.SiO_2.Al_2O_3 + 5.25051E-005 \text{ x } CaO.CaF_2.Al_2O_3\end{aligned} \tag{12}$$

3.2 Effect of Flux Ingredients on delta Quantities in Series of Weld Bead Deposits

Maximum carbon content observed in the base metal and filler wire is 0.063 and 0.029 (Table 2) while the maximum expected weld bead carbon content (0.0592) was observed for

Table 4 Dilution values and chemical composition of weld bead

			Expected weld bead content (%)								
Flux	D	D-1	C	Si	P	S	Mn	Ni	Cr	Mo	CE
f1	0.31	0.69	0.0515	0.2570	0.0221	0.0015	0.9876	0.0110	0.0633	0.3391	0.30
f2	0.28	0.72	0.0561	0.3425	0.0168	0.0020	0.9994	0.0098	0.0646	0.2893	0.29
f3	0.38	0.62	0.0442	0.3877	0.0209	0.0030	0.7543	0.0100	0.0604	0.3071	0.24
f4	0.29	0.71	0.0425	0.5439	0.0203	0.0037	0.5788	0.0096	0.0581	0.2821	0.21
f5	0.26	0.74	0.0542	0.4240	0.0184	0.0026	0.8769	0.0095	0.0627	0.2952	0.27
f6	0.30	0.70	0.0513	0.3735	0.0195	0.0056	0.7271	0.0101	0.0626	0.2876	0.24
f7	0.20	0.80	0.0470	0.3935	0.0174	0.0050	0.7337	0.0108	0.0627	0.2842	0.24
f8	0.34	0.66	0.0443	0.4654	0.0249	0.0065	0.7447	0.0099	0.0647	0.3025	0.24
f9	0.24	0.76	0.0483	0.3975	0.0237	0.0082	0.7449	0.0099	0.0667	0.2892	0.24
f10	0.19	0.81	0.0475	0.3692	0.0202	0.0045	0.7596	0.0105	0.0653	0.2970	0.25
f11	0.16	0.84	0.0422	0.5871	0.0215	0.0044	0.5813	0.0103	0.0599	0.3151	0.21
f12	0.25	0.75	0.0566	0.2797	0.0196	0.0020	1.0671	0.0099	0.0730	0.2762	0.30
f13	0.21	0.79	0.0483	0.5519	0.0208	0.0062	0.6837	0.0103	0.0653	0.2842	0.23
f14	0.15	0.85	0.0592	0.4519	0.0224	0.0059	0.7608	0.0103	0.0644	0.3183	0.26
f15	0.32	0.68	0.0562	0.3462	0.0206	0.0034	0.9887	0.0106	0.0676	0.3082	0.30
f16	0.40	0.60	0.0501	0.4239	0.0219	0.0043	0.8652	0.0107	0.0695	0.2966	0.27
f17	0.27	0.73	0.0489	0.5227	0.0221	0.0045	0.7110	0.0107	0.0672	0.2923	0.24
f18	0.36	0.64	0.0458	0.5686	0.0213	0.0057	0.5816	0.0109	0.0618	0.3127	0.22
f19	0.41	0.59	0.0459	0.4622	0.0230	0.0031	0.8116	0.0106	0.0699	0.2764	0.25
f20	0.21	0.79	0.0471	0.5480	0.0187	0.0059	0.6590	0.0104	0.0701	0.2610	0.22
f21	0.44	0.56	0.0516	0.4653	0.0186	0.0047	0.8487	0.0090	0.0718	0.2725	0.28

Table 5 Observed values as well as (Δ) transfer quantities by flux

Flux	ΔC	ΔSi	ΔMn	ΔP	ΔS	ΔMo	ΔNi	ΔCr
f1	0.01196	0.09677	−0.12179	0.01303	−0.00364	0.18975	−0.14554	0.03936
f2	0.01758	0.18926	−0.08692	0.00764	−0.00332	0.1335	−0.13972	0.03988
f3	0.00228	0.21116	−0.40892	0.01204	−0.00172	0.1728	−0.16292	0.03828
f4	0.00364	0.38833	−0.51521	0.01117	−0.00156	0.12845	−0.14226	0.03364
f5	0.01636	0.27542	−0.19404	0.00918	−0.00284	0.1351	−0.13534	0.03746
f6	0.0121	0.2156	−0.3746	0.0104	0.0004	0.1361	−0.1441	0.0384
f7	0.0112	0.2589	−0.2911	0.008	−0.0008	0.1112	−0.12	0.0359
f8	0.00374	0.29818	−0.38776	0.01592	0.00154	0.1596	−0.15366	0.04154
f9	0.01114	0.25358	−0.31066	0.01442	0.00264	0.1248	−0.13026	0.04094
f10	0.01204	0.23693	−0.25751	0.01077	−0.00136	0.12185	−0.11796	0.03824
f11	0.00776	0.46182	−0.41274	0.01198	−0.00164	0.1335	−0.11114	0.03206
f12	0.0191	0.13345	0.00385	0.01035	−0.0035	0.11395	−0.1326	0.0475
f13	0.01216	0.41497	−0.34879	0.01143	0.00046	0.11335	−0.12284	0.03876
f14	0.0251	0.32895	−0.22555	0.01285	−0.0002	0.13455	−0.1088	0.0363
f15	0.01632	0.18364	−0.12838	0.01156	−0.00168	0.161	−0.14828	0.04392
f16	0.0075	0.2427	−0.3134	0.0131	−0.0003	0.1666	−0.1669	0.0479
f17	0.01072	0.37179	−0.36763	0.01291	−0.00088	0.13435	−0.13648	0.04222
f18	0.00456	0.39672	−0.56624	0.01238	0.00086	0.1741	−0.15734	0.03916
f19	0.00296	0.27867	−0.37469	0.01423	−0.00144	0.14855	−0.16934	0.04856
f20	0.01096	0.41107	−0.37349	0.00933	0.00016	0.09015	−0.12274	0.04356
f21	0.00764	0.27478	−0.36066	0.00992	0.00034	0.1511	−0.17796	0.05124

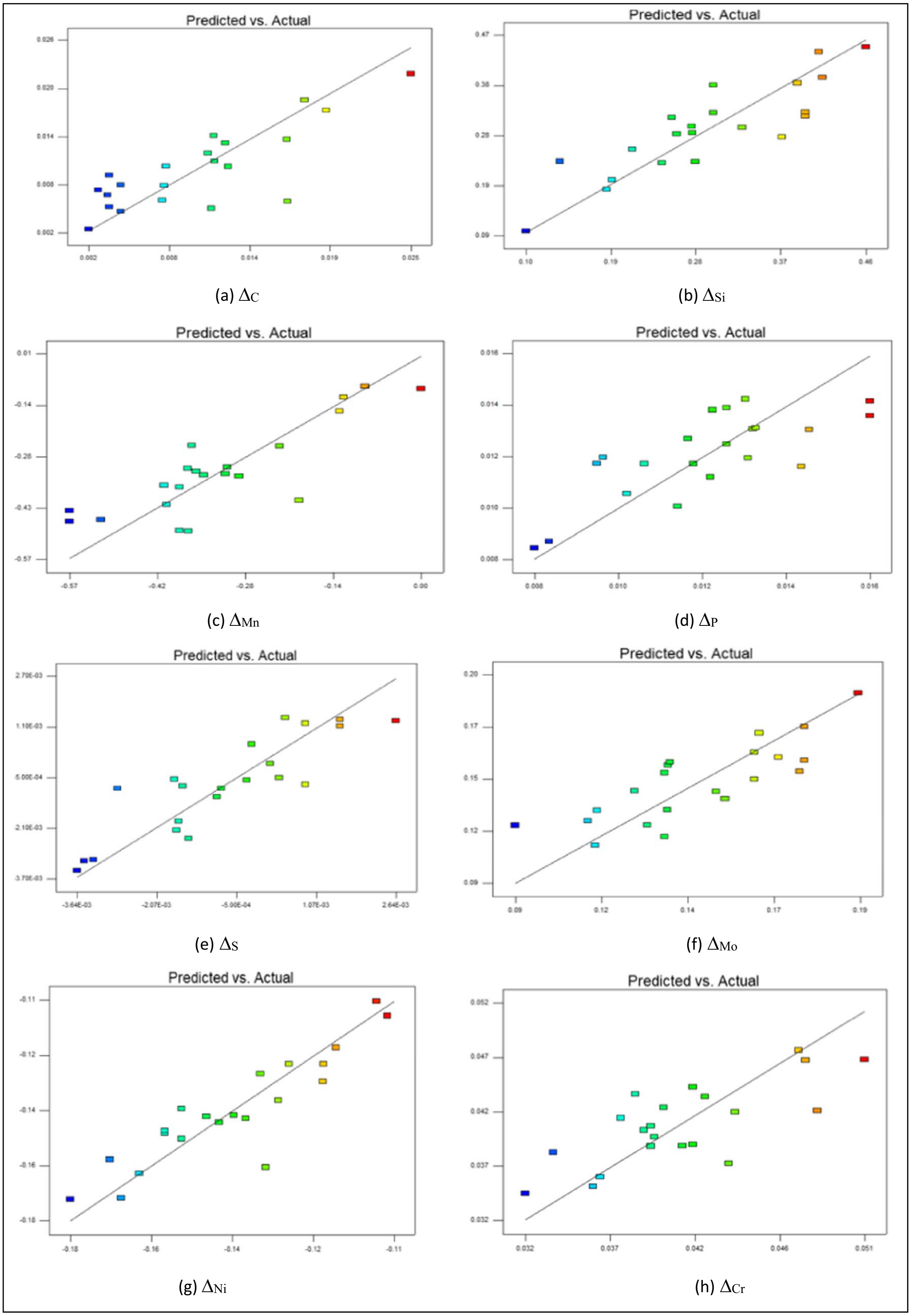

Fig. 3 Predicted vs. actual plots of delta quantities for various responses in series of weld deposits

Table 6 ANOVA results

Properties	*Source*	*SS*	*DOF*	*MSS*	*F value*	*P value*	*R^2 value*	*Significant*
Δ_C	Model	0.21	8	0.013	3.12	0.0258	0.75	Significant
	Linear	0.025	3	0.011	2.10	0.8338		
	K.L	0.023	1	0.052	4.20	0.2850		
	K.M	0.050	1	0.050	3.02	0.5203		
	K.N	0.062	1	0.051	4.00	0.5182		
	L.M	0.052	1	0.013	2.01	0.6252		
	L.N	0.056	1	0.056	3.05	0.8185		
	M.N	0.082	1	3.529E-002	5.02	0.6255		
	K.L.M	0.20	1	0.012	5.55	0.6472		
	K.L.N	0.38	8	0.015	4.25	0.8288		
	K.M.N	0.029	3	0.042	3.52	0.7162		
	L.M.N	0.034	1	0.028	4.22	0.8130		
	Residual	0.042	12	0.028				
	Total		20					
Δ_{Si}	Model	5.395E-002	14	7.203E-004	6.23	0.0030	0.92	Significant
	Linear	2.233E-004	2	5.365E-004	5.30	0.0230		
	K.L	3.122E-003	2	4.222E-003	2.77	0.0530		
	K.M	3.220E-002	1	4.210E-002	2.11	0.0350		
	K.N	1.133E-004	1	6.223E-004	1.82	0.0420		
	L.M	2.235E-005	1	2.235E-005	1.22	0.0275		
	L.N	8.234E-004	1	3.234E-004	1.33	0.0208		
	M.N	2.273E-004	1	5.273E-004	1.82	0.0120		
	Residual	6.223E-003	1					
	Total		20					
Δ_{Mn}	Model	0.11	10	0.020	2.36	0.0128	0.88	Significant
	Linear	0.024	2	0.021	5.20	0.0135		
	K.L	0.013	1	0.044	4.23	0.0275		
	K.M	0.080	1	0.039	1.33	0.0185		
	K.N	0.037	1	0.054	1.85	0.0180		
	L.M	0.053	1	0.018	4.20	0.0352		
	L.N	0.093	1	0.056	2.88	0.0265		
	M.N	0.068	1	0.087	4.22	0.0366		
	K.L.M	0.63	1	0.024	4.85	0.0652		
	K.L.N	0.28	1	0.028	3.54	0.0572		
	K.M.N	0.024	1	0.092	2.01	0.0755		
	L.M.N	0.053	1	0.075	2.55	0.0276		
	Residual	0.048	1	0.068				
	Total	0.31	20					
Δ_P	Model	2.230E-004	9	7.520E-004	1.23	0.0123	0.86	Significant
	Linear	1.320E-005	3	2.520E-005	1.50	0.0223		
	K.L	8.652E-003	2	8.520E-003	3.20	0.0882		
	K.M	7.236E-005	1	7.360E-005	6.20	0.0770		
	K.N	4.560E-004	1	3.630E-004	7.10	0.0228		
	L.M	1.450E-005	1	1.850E-006	4.30	0.0796		
	L.N	1.087E-004	1	1.820E-006	8.20	0.0632		
	M.N	1.890E-004	1	1.799E-005	1.20	0.0530		
	K.L.M	6.880E-003	1	5.962E-005	1.30	0.0421		
	K.L.N	1.550E-002	1	1.752E-005	2.37	0.128		
	K.M.N	3.620E-003	1	1.540E-006	2.35	0.0171		
	L.M.N	1.360E-003	1	1.532E-003	2.66	0.0147		
	Residual	4.872E-003	1	1.230E-002				

Table 6 (continued)

Properties	*Source*	*SS*	*DOF*	*MSS*	*F value*	*P value*	*R^2 value*	*Significant*
	Total		20					
Δ_S	Model	0.0402	8	0.120	3.70	0.0310	0.70	Significant
	Linear	0.0511	3	0.360	1.30	0.0133		
	K.M	0.0833	1	0.027	4.50	0.0175		
	K.N	0.0736	1	0.078	8.41	0.0140		
	M.N	0.0642	1	0.092	6.20	0.0160		
	K.M.N	0.0210	1	0.071	1.20	0.0130		
	Residual	0.0135	1	0.085				
	Total		20					
Δ_{Mo}	Model	0.0237	7	0.736	6.20	0.0030	0.85	Significant
	Linear	0.0782	2	0.632	7.11	0.0270		
	K.M	0.0752	1	0.023	4.20	0.0740		
	K.N	0.0423	1	0.410	1.20	0.0410		
	M.N	0.0482	1	0.012	3.20	0.0320		
	K.M.N	0.8230	1	0.024	3.40	0.2030		
	Residual	0.0752	1	0.082				
	Total		20					
Δ_{Ni}	Model	6.201E-003	14	0.236	3.88	0.0450	0.72	Significant
	Linear	5.555E-004	4	0.850	4.33	0.0230		
	K.L	9.210E-003	2	0.723	5.33	0.0256		
	K.M	0.0273	1	0.123	5.71	0.3200		
	K.N	0.0289	1	0.023	6.22	0.5620		
	L.M	0.3601	1	0.630	7.88	0.0850		
	K.L.M	0.0823	1	0.052	8.22	0.3020		
	K.L.N	0.0785	1	0.074	2.22	0.0251		
	Residual	8.170E-003	1	0.082				
	Total		20					
Δ_{Cr}	Model	0.2355	12	0.631	1.36	0.0452	0.71	Significant
	Linear	0.3663	2	0.821	2.35	0.0530		
	K.L	0.2855	1	0.714	2.88	0.0263		
	K.M	9.230E-003	1	0.462	1.88	0.0250		
	K.N	0.8523	1	0.253	5.20	0.0251		
	L.M	0.0536	1	0.023	1.80	0.0244		
	L.N	0.0562	1	0.082	1.40	0.4630		
	K.L.M	0.8530	1	0.840	2.36	0.2852		
	K.L.N	0.0550	1	0.052	1.25	0.8520		
	K.M.N	0.3620	1	0.025	1.85	0.2600		
	L.M.N	0.0522	1	0.025	1.33	0.7532		
	Residual	0.9630	1	0.230				
	Total		20					

flux 14 (Table 4). Although the weld bead carbon content for all the fluxes has been increased while it is lower than that of base metal. From regression Eq. 3 it has been observed that individual flux ingredients **CaO, SiO_2, CaF_2** and **Al_2O_3** incresars the delta carbon content. Binary interations such as **CaO.SiO_2, CaO.CaF_2, CaO.Al_2O_3, SiO_2.CaF_2** and **CaF_2.Al_2O_3** shows the significant negative effect on delta carbon content. The CaO.SiO_2.CaF_2 is the only ternary interction whch gives the negative effect while **CaO.SiO_2.Al_2O_3** and **CaO.CaF_2.Al_2O_3** interaction provide positive effect on delta carbon content (Eq. 3). The increase of weld bead carbon content may be due to reduction of carbon into its oxides during slag-metal interactions becaue in high temperature region flux ingreditents such as **CaO, SiO_2** and **Al_2O_3** decomposed to release the free oxygen ions. These free oxygen ions (O^-) react with the carbon ions from the parent as well as filler metal and forming its oxides [24–26]. From results it has been noticed that weld bead silicon content significantly increseased from the parent metal

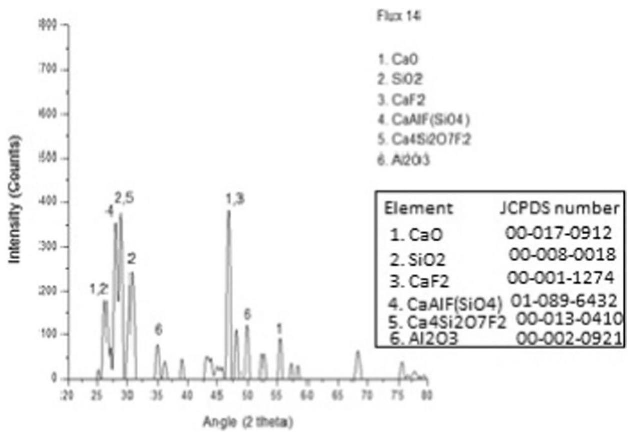

Fig. 4 XRD analysis

as well as of filler wire (Tables 2, 4 and 5). All the individual flux ingredients decreseas the weld bead delta silicon content while all the binary interactions increases the weld bead delta silicon content (Eq. 4). The negative effect of individual flux ingredients on Δ_{Si} content may be due to the formation of silicates or other complex compounds which was cross checked by XRD analysis of the flux specimen as shown in Fig. 4. The incease of Δ_{Si} in the weld bead may be due to the presence of SiO_2in the flux which dissociates in free silicon and oxygen ions in weld pool region. CaO has insignificant role in increasing the weld bead Δ_{Si} content because calcium oxide dissociates to $\mathbf{Ca^{++}}$ ions and free oxygen ions which in turns react with free silicon ions present in the arc region and forms $\mathbf{SiO_2}$ and calcium react with oxygen and again form **CaO** [27–30].

Maximum value of manganese in base metal is 1.640 while in filler it is 0.871. From Table 4 it has been observed that for all the experiments there is decrease in Δ_{Mn} content in weld bead deposits. From Eq. 5 it has been noticed that primary flux ingredients **CaO, $\mathbf{SiO_2}$, $\mathbf{CaF_2}$** and $\mathbf{Al_2O_3}$ increases the weld bead Δ_{Mn} content while all the secondary flux interactions decreases the weld bead Δ_{Mn} content. $\mathbf{CaO.SiO_2.CaF_2}$ is the only ternary interaction which decreases the Δ_{Mn} content while remaining all shows positive effect on Δ_{Mn} and increases its weld bead content. Previous literature suggests that transfer of manganese basically depends upon the flux and filler wire composition [31, 32]. Increase in delta phosphorous content in the weld bead specimen is basically indicates that there is increase in strength for all the specimens but at the same time there are chances of increase in crack sensitivity because it act as an impurity in the weld region [33]. From regression Eq. 6 it is clear that primary flux ingredients such as **CaO, $\mathbf{SiO_2}$** and $\mathbf{CaF_2}$ tends to increase the Δ_P content while $\mathbf{Al_2O_3}$ decreases Δ_P content in weld bead region. All the secondary flux interactions gives positive effect on Δ_P and increases its value in the weld region expect $\mathbf{CaO.SiO_2}$ and $\mathbf{SiO_2.CaF_2}$ interaction. All the ternary flux mixture interactions gives negative effect on Δ_P and thus significantly reduces its value in the weld region except $\mathbf{CaO.SiO_2.CaF_2}$ interaction. From Table 5 it has been noticed that there is a gain in sulphur content for flux specimen 6, 8, 9, 13, 18, 20 and 21 while for remaining specimen there is loss in sulphur content. From Eq. 7 it is noticed that all the primary flux elements tends to decrease the Δ_S content while all the secondary flux mixture interactions tends to give positive effect on Δ_S and increases its value. Available literature suggests that weld impurities are well addressed by lime fluxes, because when calcium oxide reacts with sulphur it forms calcium sulphide (CaS) and free oxygen by lowering the sulphur content in the weld region [34]. There is significant increase in Δ_{Mo} content for all the experiments (Table 4). **CaO** and $\mathbf{SiO_2}$ has positive effect on Δ_{Mo} and increases its content in weld region while CaF_2 and Al_2O_3 shows negative effect on Δ_{Mo} and decreases its content in weld region. Increase in Δ_{Mo} content may be basically due to the electrochemical interactions taking place at the parent metal [35]. From Table 5 it has been noticed that there is significant decrease in Δ_{Ni} content for all the experiments. Primary flux components such as **CaO, $\mathbf{SiO_2}$ and $\mathbf{CaF_2}$** significantly reduces Δ_{Ni} content while $\mathbf{Al_2O_3}$ increases the weld bead nickel content. Only $\mathbf{CaO.Al_2O_3}$ and $\mathbf{SiO_2.Al_2O_3}$ binary flux components reduces the nickel content while all of the rest mixture interactions increases weld bead nickel content. $\mathbf{CaO.SiO_2.CaF_2}$ ternary interaction tends to decrease the weld bead nickel content and thus having negative effect on Δ_{Ni} while $\mathbf{CaO.SiO_2.Al_2O_3}$ shows positive effect on it (Eq. 9). From Table 5 it has been noticed that there is significant increase in Δ_{Cr} content for all the experiments. Chromium is a strong carbide forming element and is also responsible for reducing the corrosion behaviour of low alloys steels. All the primary flux components tends to increase the Δ_{Cr} content for all specimens. **CaO** and $\mathbf{CaF_2}$ from flux react with chromium present in base and filler metal and will form chromium oxide and free oxygen and fluorine. Free oxygen and fluorine again re-react with the calcium ions ($\mathbf{Ca^{++}}$) present in the molten pool to form **CaO** and $\mathbf{CaF_2}$ [36].

3.3 Microstructure Analysis

Microstructure of some of the weld beads were analysed to verify the presence of carbide inclusions using optical microscope. API X70 weld metal basically exhibit acicular ferrite microstructure with some inclusions of carbides dispersed in it [37]. From Table 5 it has been noticed that carbon content in the weld bead significantly

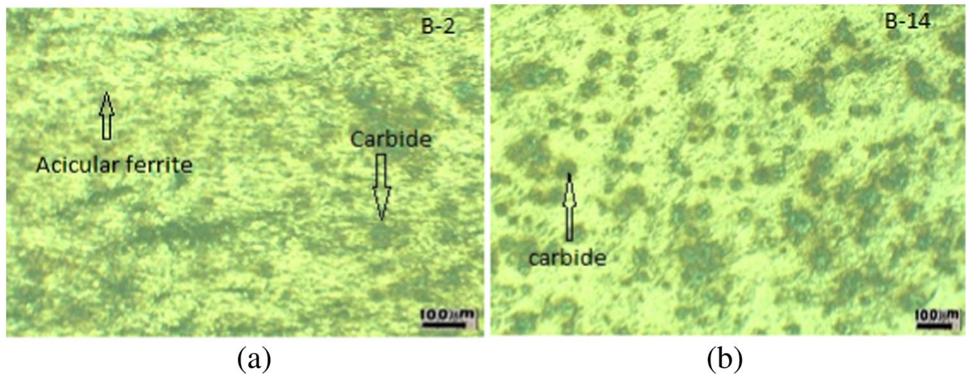

Fig. 5 a-b: Microstructure of weld beads

increased which is verified from the micrographs shown in Fig. 5. From Fig. 5a-b it can be seen that most of the carbon particles are dispersed as inclusions in the matrix. Figure 6 shows the SEM plots of B-2 flux at higher magnifcation which clearly shows the formation of acicular ferrite phase and other micro inclusions such chromium, nickel and mangnese. From SEM plots it has been clearly observed that these carbide as inclusions are dispered in the acicular ferrite matrix.

3.4 Curvation for Different Responses

Variation in change in Δ element has been observed on the different regions on contour curves. Variation in the element transfer can be observed on the surface of the contour curve which gives the constant value of Δ while flux mixture combination was well seen by dotted points on the curves [38]. Curves indicating the predicted values for different responses such as Δ_C, Δ_{Si}, Δ_{Mn}, $\Delta_{P,}$ Δ_S, Δ_{Mo}, Δ_{Ni} and Δ_{Cr} are shown in Fig. 7.

3.5 Optimization & Validation of Model

To optimize the Δ quantities of weld beads similar to the base metal an attempt has been made. To simultaneously optimize all the responses a compound desirability optimization technique used which was given by derringer and suich [39]. Table 7 represents the desirability values of different Δ quantities. To find the error (E) values of different Δ responses, 3 flux compositions with larger desirability value was chosen for the study [40–42]. Table 8 represents percentage error values for different Δ responses.

4 Conclusion

- Weld bead carbon content for all the experiments has been increased while it is lower than that of base metal. Maximum carbon content observed in the base metal and filler wire was 0.063 and 0.029. Flux number 14 (0.0592) shows the maximum increase in weld bead crabon content as compared to the remaining fluxes.

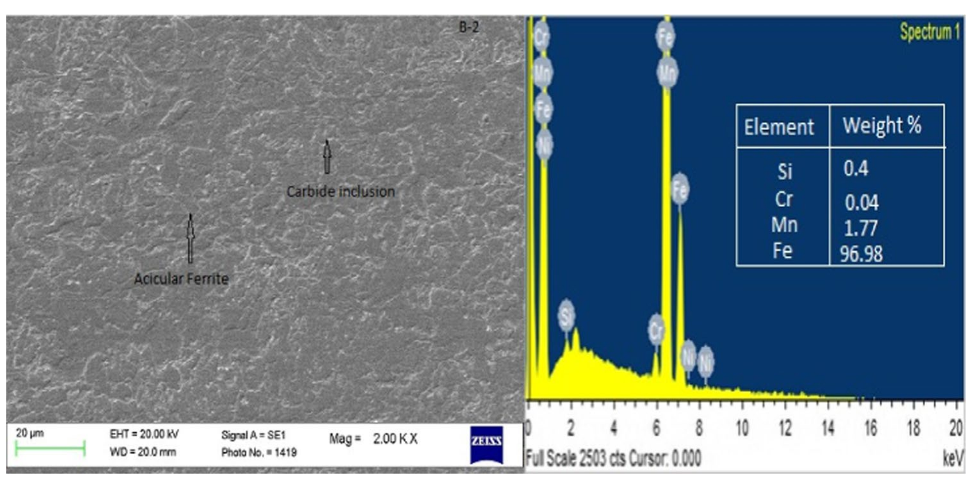

Fig. 6 SEM plot of B-2 flux

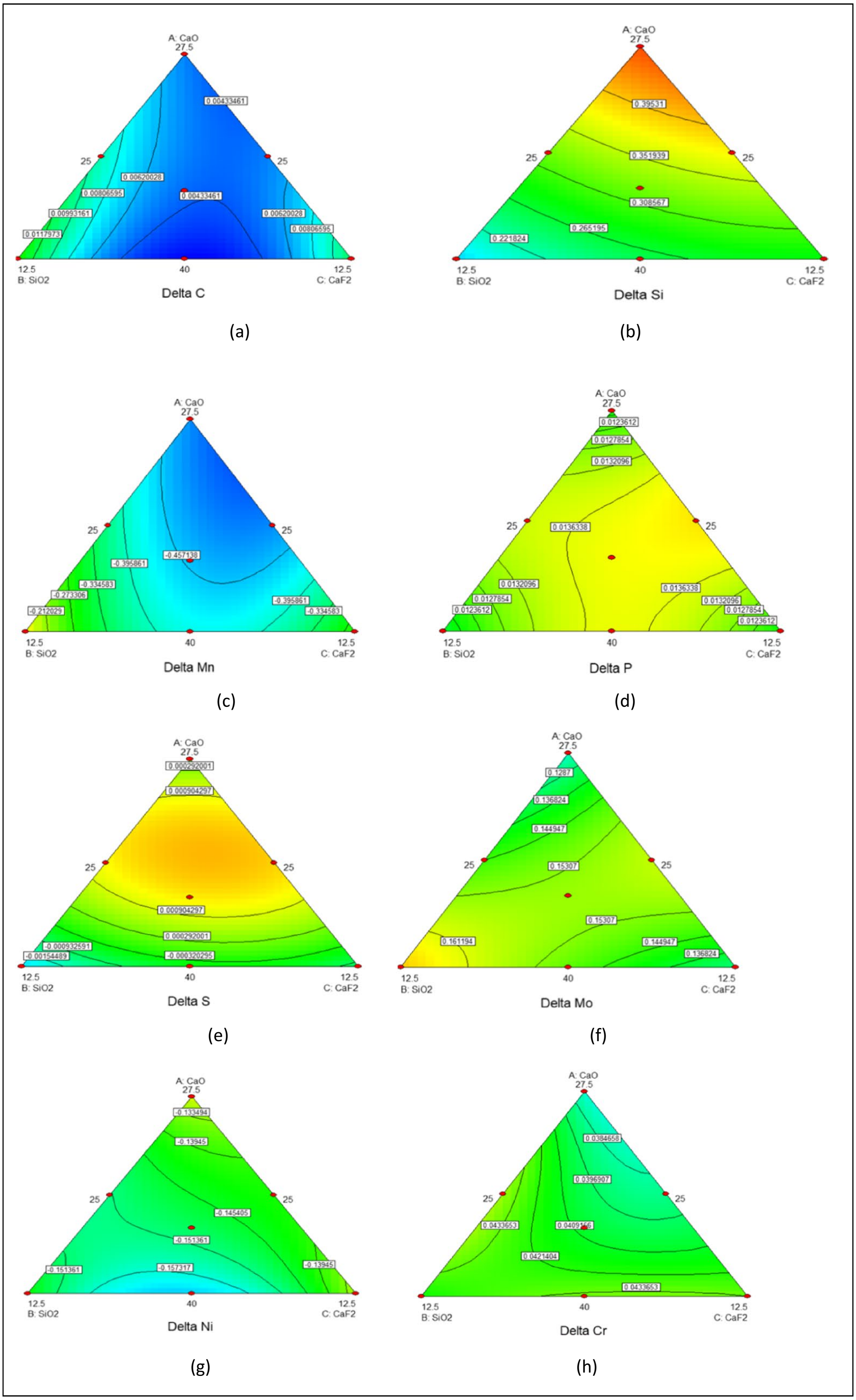

Fig. 7 Curves for different Δ transfer responses

Table 7 Desired values of different Δ responses

S.No	CaO	SiO_2	CaF_2	Al_2O_3	Δ_C	Δ_{Si}	Δ_{Mn}	Δ_P	Δ_S	Δ_{Mo}	Δ_{Ni}	Δ_{Cr}	Desirability
1	40.1	10.1	25.1	10.1	0.01196	0.09677	−0.12179	0.01303	−0.00364	0.18975	−0.14554	0.03936	0.85
2	30.1	25.1	25.1	5.1	0.00364	0.38833	−0.51521	0.01117	−0.00156	0.12845	−0.14226	0.03364	0.75
3	33.57	18.57	25.1	7.4	0.00374	0.29818	−0.38776	0.01592	0.00154	0.1596	−0.15366	0.04154	0.83

Table 8 % error values for $\Delta_{C,}$ $\Delta_{Si,}$ Δ_{Mn} & Δ_P responses

Flux Components				PV				AV				E			
CaO	SiO_2	CaF_2	Al_2O_3	Δ_C	Δ_{Si}	Δ_{Mn}	Δ_P	Δ_C	Δ_{Si}	Δ_{Mn}	Δ_P	Δ_C	Δ_{Si}	Δ_{Mn}	Δ_P
40.1	10.1	25.1	10.1	0.01192	0.09599	−0.12180	0.01304	0.01196	0.09677	−0.12179	0.01303	0.98	0.90	0.87	0.98
30.1	25.1	25.1	5.1	0.0062	0.38822	−0.51511	0.0118	0.00364	0.38833	−0.51521	0.01117	0.99	0.61	0.48	1.03
33.57	18.57	25.1	7.4	0.00375	0.29819	−0.38778	0.01595	0.00374	0.29818	−0.38776	0.01592	0.99	0.70	0.82	0.88

- All the individual flux ingredients decreseas the weld bead delta silicon content while all the binary interactions increases the weld bead delta silicon content. The negative effect of individual flux ingredients on Δ_{Si} content due to the formation of silicates or other complex compounds while the incease of Δ_{Si} in the weld bead may be due to the presence of SiO_2 in the flux which dissociates in free silicon and oxygen ions in weld pool region.
- For all the experiments there is decrease in Δ_{Mn} content in weld bead deposits. Individual flux ingredients **CaO, SiO_2, CaF_2** and **Al_2O_3** increases the weld bead Δ_{Mn} content while all the binary flux interactions decreases the weld bead Δ_{Mn} content.
- Individual flux ingredients such as **CaO, SiO_2** and **CaF_2** tends to increase the Δ_P content and shows synergistic effect while Al_2O_3 decreases Δ_P content in weld bead region and gives antisynergistic effect on it. Increase in Δ_P content in the weld bead specimen is basically indicates that there is increase in strength for all the specimens.
- There is a gain in sulphur content for flux specimen 6, 8, 9, 13, 18, 20 and 21 while for remaining specimen there is loss in sulphur content.
- **CaO** and **SiO_2** has positive effect on Δ_{Mo} and increases its content in weld region while CaF_2 and Al_2O_3 shows negative effect on Δ_{Mo} and decreases its content in weld region.
- For all experiments there is significant increase in Δ_{Cr} content.

Acknowledgements It is requested to editorial board to please acknowledge the present research for possible publication in Silicon journal. The content is new and unpublished.

Authors' Contributions It is certified on behalf of corresponding author (Lochan Sharma) that all authors are equally contributed in the present manuscript.

Funding It is certified on behalf of corresponding author (Lochan Sharma) that present research is not funded by any external agency.

Data Availability I Lochan Sharma (Corresponding Author) certified that data & material will be available on author's request.

Declarations

Ethical Approval I Lochan Sharma (Corresponding Author) on behalf of other co-authors certified that I have taken the ethical approval to publish the data presented in the manuscript. Also the data used in this manuscript (such as figures) has been cited in this paper.

Consent to Participate NA.

Consent of Publication I Lochan Sharma (Corresponding Author) on behalf of other coauthors certified that I have taken the permission to publish the present content.

Competing Interests It is certified on behalf of corresponding author (Lochan Sharma) that present research is not funded by any external agency and authors declared that there is no conflicts of interest in the present research.

Conflict of Interest It is certified on behalf of corresponding author (Lochan Sharma) that present research is not funded by any external agency and authors declared that there is no conflicts of interest in the present research.

Research Involving Human Participants and/or Animals The present research is involved for human participants.

Informed Consent NA.

References

1. Grey JM (2002) An independent view of linepipe and linepipe steel for high strength pipelines. Microalloying International, LP, Houston, Texas, X80 Pipeline Cost Workshop. 8:1–19
2. Piper J (2002) X80 line pipe for small diameter (DN450 and smaller) high strength pipelines. Nippon Steel Corporation and Kawasaki Steel Corporation 41:35
3. Ragu Nathan S, Balasubramanian V, Malarvizhi S, Rao A. G (2015) Effect of welding processes on mechanical and microstructural characteristics of high strength low alloy naval grade steel joints. Def Technol 11:308–317
4. Serindag HT, Tardu C, Kircicek IO, Cam G (2022) A study on microstructural and mechanical properties of gas tungsten arc welded thick cryogenic 9% Ni alloy steel butt joint. CIRP J Manuf Sci Technol 37:1–10. https://doi.org/10.1016/j.cirpj.2021.12.006
5. H.T. Serindag and G. Cam, Microstructure and mechanical properties of gas metal arc welded AISI 430/AISI 304 dissimilar stainless steels butt joints, J Phys Conf Ser, Vol. 1777, 2021, Paper No: 012047 https://doi.org/10.1088/1742-6596/1777/1/012047
6. Liu S, Fredrickson GL, Johnson MQ, Edwards GR (1992) Shielded metal arc welding consumables for advanced high strength steels, work performed under contract N00014-89-j-3170, annual progress report. Centre for Welding and Joining Research Colorado School of Mines, Colorado, pp 1–82
7. Murugan N, Gunaraj V (2005) Prediction and control of weld bead geometry and shape relationships in submerged arc welding of pipes. J Mater Process Tech 168:478–487
8. Hashemi SH, Mohammadyani D (2012) Characterisation of weldment hardness, impact energy and microstructure in API X65 steel. Int J Press Vessel Pip 98:8–15
9. Kanjilal P, Pal TK, Majumdar SK (2006) Combined effect of flux and welding parameters on chemical composition and mechanical properties of submerged arc weld metal. J Mater Process Tech 171:223–231
10. O'Brien A, Guzman C (2004) Welding handbook: welding processes, part 2. American Welding Society, Miami, FL
11. Olson DL, Frost RH (1991) Welding and joining processes. American Society of Mechanical Engineers 18:1–6
12. Liu S, Olson DL (1987) The influence of inclusion chemical composition on weld metal microstructure. Journal of Materials Engineering 9:237–251. https://doi.org/10.1007/BF02834144
13. Barritte GS, Edmonds DV (1981) Proceedings conference on advances in the physical metallurgy of steel. The Metals Society, London
14. Waris KN, Rahul C (2021) Experimental investigation on dissimilar weld between super duplex stainless steel 2507 and API X70 pipeline steel. Proceedings of the Institution of Mechanical Eng Part J Mater Des Appl 235(8). https://doi.org/10.1177/14644207211013056
15. Waris KN, Rahul C (2021) Characterization of CaO-CaF2-TiO2-SiO2 Based Welding Slags for Physicochemical and Thermophysical Properties. Silicon 13(7). https://doi.org/10.1007/s12633-020-00537-8
16. Sumit M, Waris KN, Rahul C (2021) CaO-CaF2-SiO2-Al2O3 system for development of SMAW electrodes with Ni alloy core wire. Ceram Int 47(8). https://doi.org/10.1016/j.ceramint.2021.03.042
17. Waris KN, Rahul C (2021) Investigations on effect of CaO-CaF2-TiO2-SiO2 based electrode coating constituents and their interactions on weld chemistry. Ceram Int 47(2). https://doi.org/10.1016/j.ceramint.2021.01.106
18. Sumit M, Jagdish K, Rahul C (2020) High-temperature wettability investigations on laboratory-developed CaO-CaF2-SiO2 -Al2O3 flux system-based welding electrode coatings for power plant applications. Silicon. https://doi.org/10.1007/s12633-019-00374-4
19. Biswas A, Bhowmik A (2018) Study of heat generation and its effect during submerged arc welding (SAW) on mild steel plate at zero degree Celsius plate temperature. Materials Today: Proceedings 5(5):13400–13405
20. Cornell JA (2011) Experiments with mixtures: designs, models, and the analysis of mixture data. Wiley, New York
21. Eriksson G, Pelton AD (1993) Critical evaluation and optimization of thermodynamic properties and phase diagrams of the CaO-Al_2O_3, Al_2O_3-SiO_2 and CaO- SiO_2-Al_2O_3 systems.Met mater. Trans B 24:807–816
22. Sharma L, Chhibber R (2019) Design of CaO-SiO_2-CaF_2 and CaO-SiO_2-Al_2O_3 based submerged arc fluxes for series of bead on plate pipeline steel welds : effect on carbon and manganese content. Grain size and Microhardness, J Pressure Vessel Technol, ASME 141:1–10
23. Anderson VL, McLean RA (1974) Design of experiments: a realistic approach. Marcel Dekker, Inc., New York
24. Mitra U, Eagar TW (1984) Slag metal reactions during submerged arc welding of alloy steels. Metall Trans A 15:217–227
25. Kanjilal P, Majumdar SK, Pal TK (2005) Prediction of acicular ferrite from flux ingredients in submerged arc weld metal of C-Mn steel. ISIJ Int 45:876–885
26. Pandey ND, Bharti A, Gupta SR (1994) Effect of submerged arc welding parameters and fluxes on element transfer behaviour and weld-metal chemistry. J Mater Process Tech 40:195–211
27. Kanjilal P, Pal TK, Majumdar SK (2007) Prediction of element transfer in submerged arc welding. Weld J 86:135s–146s
28. Burck PA, Indacochea JE, Olson DL (1990) Effects of welding flux additions on 4340 steel weld metal composition. Weld J 3:115–122
29. Chai CS, Eagar TW (1980) The effect of SAW parameters on weld metal chemistry. Weld J 59:93s–98s
30. Jindal S, Chhibber R, Mehta NP (2013) Investigation on flux design for submerged arc welding of high-strength low-alloy steel. Proc IMechE, Part B: J Engineering Manufacture 227:383–395
31. Chang K-L, Huang C-T, Huang W et al (2008) Investigations of microstructure and phosphorus distribution in BOF slag. China Steel Tech Rep 21:1–6
32. Bhandari D, Chhibber R, Arora N (2012) Effect of electrode coatings on diffusible hydrogen content, hardness and microstructures of the ferritic heat affected zones in bimetallic welds. Adv Mater Res 383:4697–4701
33. Singh K, Pandey S (2008) Economics of recycling submerged arc welding slag as a flux, Proceedings of the 8th international conference on trends in welding research, Pine Mountain, GA. ASM International, Materials Park, pp 806–810
34. Jindal S, Chhibber R, Mehta NP (2014) Effect of welding parameters on bead profile, microhardness and H2 content in submerged arc welding of high-strength low-alloy steel. Proc IMechE, Part B: J Eng Manuf 228:82–94
35. Paniagua-Mercado AM, Lopez-Hirata VM (2011) Chemical and physical properties of fluxes for SAW of low-carbon steels. Arc Weld 13:281–298
36. Du Plessis J, du Toit M, Pistorius PC (2007) Control of diffusible weld metal hydrogen through flux chemistry modification. Weld J 86:273s–280s

37. Ramirez JE (2008) Characterization of high-strength steel weld metals: chemical composition, microstructure, and non-metallic inclusions. Weld J 87:65s–75s
38. Hummel FA (1984) Introduction to phase equilibrium in ceramics systems. CRC Press Ltd, Boca Raton, FL
39. Derringer G, Suich R (1980) Simultaneous optimization of several response variables. J Qual Technol 12:214–219
40. Harrington EC (1965) The desirability function. Ind Qual. Control 21:494–498
41. Bhowmik A, Biswas A (2022) Wear resistivity of Al7075/6wt.% SiC composite by using Grey-fuzzy optimization technique. Silicon 14:3843–3856
42. Bhowmik A, Dey S, Dey D, Biswas A (2021) Dry sliding Wear performance of Al7075/SiC composites by applying Grey-fuzzy approach. Silicon 13(5):1–16